

# Diffractive vector meson electroproduction at small Bjorken $x$ within GPD approach

S.V.Goloskokov <sup>a</sup>

Bogoliubov Laboratory of Theoretical Physics, Joint Institute for Nuclear Research, Dubna, Russia

**Abstract.** We study light vector meson electroproduction at small  $x$  within the generalized parton distributions (GPDs) model. The modified perturbative approach is used, where the quark transverse degrees of freedom in the vector meson wave function and hard subprocess are considered. Our results on the cross section and spin observables are in good agreement with experiment.

## 1 Introduction

Study of GPDs can give extensive information on the hadron structure. Vector meson leptoproduction at high energies [1,2,3] is one of the essential processes where the GPDs can be investigated. At small  $x$ -Bjorken the leading twist amplitude with longitudinally polarized photon and vector meson (LL amplitude) at large photon virtualities  $Q^2$  factorizes [4] into a hard meson leptoproduction off partons and GPDs. The transition amplitude for transversally polarized photons  $\gamma_\perp^* \rightarrow V_\perp$  (TT amplitude) is suppressed as a power of  $1/Q$  and its factorization is problematic. The generally used collinear approximation leads to difficulties in studying these reactions. Really the longitudinal cross section calculated in the collinear approach [5] exceeds the data by an order of magnitude. The TT amplitude exhibits infrared singularities in the collinear approach [6] which is a reason of the factorization breakdown.

These problems can be solved in handbag model [1,2] based on the modified perturbative approach (MPA) [7] which includes the quark transverse degrees of freedom accompanied by the Sudakov suppressions. They suppress the contribution from the end-point region and the LL cross section are close to the experiment. The transverse quark momentum regularizes the end-point singularities in the TT amplitudes and it can be calculated in the model. Thus, our model provides an access to study GPDs in the polarized vector meson production.

In our previous calculations [1] we analyzed the low  $x \leq 0.01$  region where the gluon contribution had a predominant role. In this report, we extend our analysis to moderate  $x \sim 0.2$  [2]. Within the MPA we calculate the LL and TT amplitudes, and afterwards the cross sections and the spin observables in the light vector meson leptoproduction. Our results are in reasonable agreement with high energy HERA experiments [8,9] and low energy HERMES [10] and E665 [11] data for electroproduced  $\rho$  and  $\phi$  mesons at small  $x$  [1,2].

## 2 Leptoproduction of Vector Mesons in the GPD approach

The model is based on the handbag approach where the  $\gamma^* p \rightarrow V p$  amplitude factorizes into hard partonic subprocess and GPDs. In the region of small  $x \leq 0.01$  the gluon GPD is a dominant contribution [1]. At larger  $x \sim 0.2$  the quark contributions are essential [2]. For small

---

<sup>a</sup> e-mail: goloskkv@theor.jinr.ru

$t$  the amplitude of the vector meson production off the proton with positive helicity reads as a convolution of the hard subprocess amplitude  $\mathcal{H}^V$  and GPDs  $H^i(\tilde{H}^i)$ :

$$\mathcal{M}_{\mu'+,\mu+}^V = \frac{e}{2} \mathcal{C}^V \sum_{\lambda} \int d\bar{x} \mathcal{H}_{\mu'\lambda,\mu\lambda}^{Vi} H^i(\bar{x}, \xi, t), \quad (1)$$

where  $i$  denotes the gluon and quark contribution,  $\mu$  ( $\mu'$ ) is the helicity of the photon (meson),  $\bar{x}$  is the momentum fraction of the parton with helicity  $\lambda$ , and the skewness  $\xi$  is related to Bjorken- $x$  by  $\xi \simeq x/2$ . The flavor factors are  $C^\rho = 1/\sqrt{2}$  and  $C^\phi = -1/3$ . The polarized GPDs  $\tilde{H}^i$  are unimportant in the analysis of the cross section because at small  $x$  they are much smaller with respect to the unpolarized GPDs  $H^i$ .

The hard part is calculated using the  $k$ - dependent wave function [12] that contains the leading and higher twist terms describing the longitudinally and transversally polarized vector mesons, respectively. The subprocess amplitude is calculated within the MPA [7]. The amplitude  $\mathcal{H}^V$  is represented as the contraction of the hard part  $F$ , which is calculated perturbatively, and the non-perturbative meson wave function  $\phi_V$

$$\mathcal{H}_{\mu'+,\mu+}^V = \frac{2\pi\alpha_s(\mu_R)}{\sqrt{2N_c}} \int_0^1 d\tau \int \frac{d^2\mathbf{k}_\perp}{16\pi^3} \phi_V(\tau, k_\perp^2) F_{\mu'\mu}^\pm. \quad (2)$$

The wave function is chosen in the Gaussian form

$$\phi_V(\mathbf{k}_\perp, \tau) = 8\pi^2 \sqrt{2N_c} f_V a_V^2 \exp \left[ -a_V^2 \frac{\mathbf{k}_\perp^2}{\tau\bar{\tau}} \right]. \quad (3)$$

Here  $\bar{\tau} = 1 - \tau$ ,  $f_V$  is the decay coupling constant and the  $a_V$  parameter determines the value of average transverse momentum of the quark in the vector meson. The values of  $f_V, a_V$  are different for longitudinal and transverse polarization of the meson.

In the hard part  $F$  we keep the  $k_\perp^2$  terms in the denominators of LL and TT transitions and in the numerator of the TT amplitude. The gluonic corrections are treated in the form of the Sudakov factors which additionally suppress the end-point integration regions.

To estimate GPDs, we use the double distribution representation [13] with the double distribution function

$$f_i(\beta, \alpha, t) = h_i(\beta, t) \frac{\Gamma(2n_i + 2)}{2^{2n_i+1} \Gamma^2(n_i + 1)} \frac{[(1 - |\beta|)^2 - \alpha^2]^{n_i}}{(1 - |\beta|)^{2n_i+1}}. \quad (4)$$

The powers  $n_i$  (i= gluon, sea, valence contributions) and the functions  $h_i(\beta, t)$  which are connected with parton distributions are determined by

$$\begin{aligned} h_g(\beta, 0) &= |\beta|g(|\beta|), & n_g &= 2; \\ h_{sea}^q(\beta, 0) &= q_{sea}(|\beta|)\text{sign}(\beta), & n_{sea} &= 2; \\ h_{val}^q(\beta, 0) &= q_{val}(\beta)\Theta(\beta), & n_{val} &= 1. \end{aligned} \quad (5)$$

Here  $g$  and  $q$  are the ordinary gluon and quark PDF. For the parton distribution the simple Regge anzats at small momentum transfer is used

$$h_i(\beta, t) = e^{b_i t} \beta^{-(\delta_i(Q^2) + \alpha'_i t)} (1 - \beta)^{2n_i+1} \sum_{j=0}^3 c_i^j \beta^{j/2}. \quad (6)$$

The  $\delta_i(Q^2)$  is connected [2] with the corresponding intercept  $\alpha_i(0)$  of the Regge trajectory  $\alpha_i = \alpha_i(0) + \alpha'_i t$ . The parameters  $c_i^j$  in (6) and there evolution are chosen by comparison with the CTEQ6M PDFs [14].

The GPDs are related with PDFs through the double distribution form

$$H_i(\bar{x}, \xi, t) = \int_{-1}^1 d\beta \int_{-1+|\beta|}^{1-|\beta|} d\alpha \delta(\beta + \xi \alpha - \bar{x}) f_i(\beta, \alpha, t). \quad (7)$$

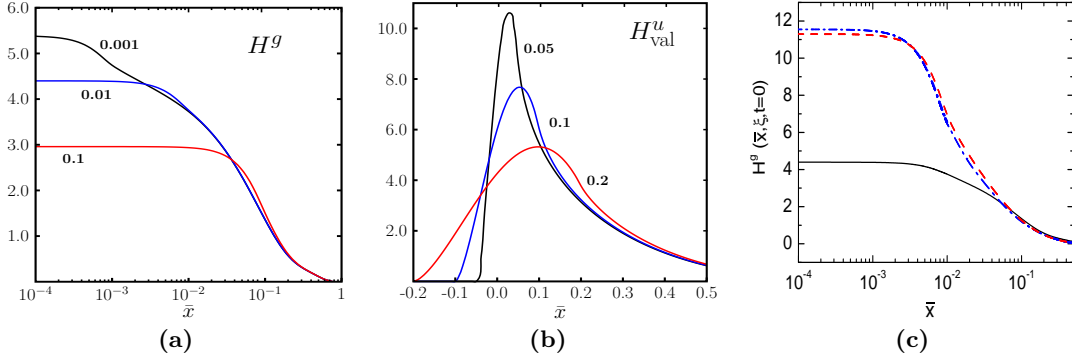


**Fig. 1.** GPDs (a)  $H^g$ , (b)  $H_{val}^u$  for some values of skewness via  $x$ . GPDs are shown at  $t = 0$  and scale  $Q^2 = 4 \text{ GeV}^2$ , (c) Evolution of gluon GPD for  $\xi = 0.01$ . Full line-  $Q^2 = 4 \text{ GeV}^2$ ;  $Q^2 = 40 \text{ GeV}^2$ : dashed-dotted line- evolution code [15], dashed line- our approximation.

The model results for the gluon and valence quark GPDs for the three  $\xi$  values are shown in Fig. 1. In our model, the GPD evolution is determined by the evolution of PDFs in (4,6). To show that we reproduce the  $Q^2$  dependence of GPDs correctly, Fig. 1c represents the results of our model and the GPDs evolution determined by evolution code [15]. Both results coincide at  $Q^2 = 4 \text{ GeV}^2$  and are close to each other at  $Q^2 = 40 \text{ GeV}^2$ .

### 3 Cross section and spin observables

In this section we study the longitudinal cross section of the vector meson production in the energy range  $5 \text{ GeV} < W < 75 \text{ GeV}$  and the spin observables at HERA energies. The  $t$ -dependence of the amplitudes is important in analyses of experimental data integrated over  $t$ . In our model, the diffraction peak slopes for LL and TT transitions are closed to each other:  $B_{LL} \sim B_{TT}$  and are determined from (6)

$$B_i = 2b_i + 2\alpha'_i \ln \frac{W^2 + Q^2}{Q^2 + m_v^2}. \quad (8)$$

For gluon and sea distributions we use  $\alpha'_g = 0.15 \text{ GeV}^{-2}$  and

$$b_{g(sea)} = 2.58 \text{ GeV}^{-2} + 0.25 \text{ GeV}^{-2} \ln \frac{m^2}{Q^2 + m^2} \quad (9)$$

which describe well the slope parameter observed experimentally. The corresponding parameters for other contributions can be found in [2].

Estimations for the light meson production amplitudes are carried out using  $f_{\rho L} = 0.209 \text{ GeV}$ ,  $a_{\rho L} = 0.75 \text{ GeV}^{-1}$ ;  $f_{\phi L} = 0.221 \text{ GeV}$ ;  $a_{\phi L} = 0.7 \text{ GeV}^{-1}$ .

At HERA energies we consider gluon and sea contributions. In this energy range, the valence quark effects can be neglected. The cross section for the  $\gamma^* p \rightarrow \rho p$  production integrated over  $t$  is shown in Fig. 2a. Good agreement with H1 and ZEUS data [8,9] is found. The typical contribution of the gluon-sea interference to  $\sigma_L$  does not exceed 45% with respect to the gluon one. It is of the order of magnitude of the uncertainties in the cross section (about 25-35 %) from the gluon GPD. The model results for the  $\phi$  production cross section shown in Fig. 2b are consistent with the experiment [8,9]. The contribution of the gluon-sea quark interference to the cross section of the  $\phi$  production does not exceed 25%.

The leading twist results, which do not take into account effects of a transverse quark motion, are presented in Fig. 2 too. One can see that the  $k_\perp^2/Q^2$  corrections in the hard amplitude are

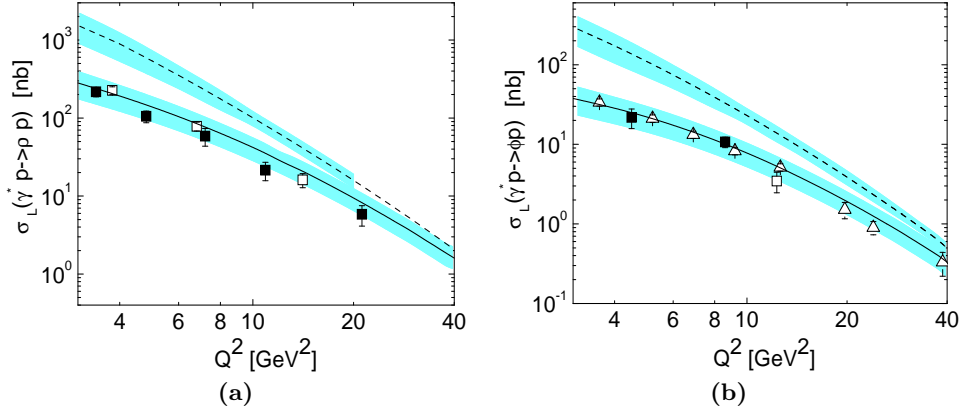


**Fig. 2.** (a) Longitudinal cross sections of  $\rho$  production at  $W = 75 \text{ GeV}$ . (b) Longitudinal cross sections of  $\phi$  production at  $W = 75 \text{ GeV}$  with error band from CTEQ6 PDFs uncertainties. Data are from H1 [8] -solid symbols and ZEUS [9] -open symbols.

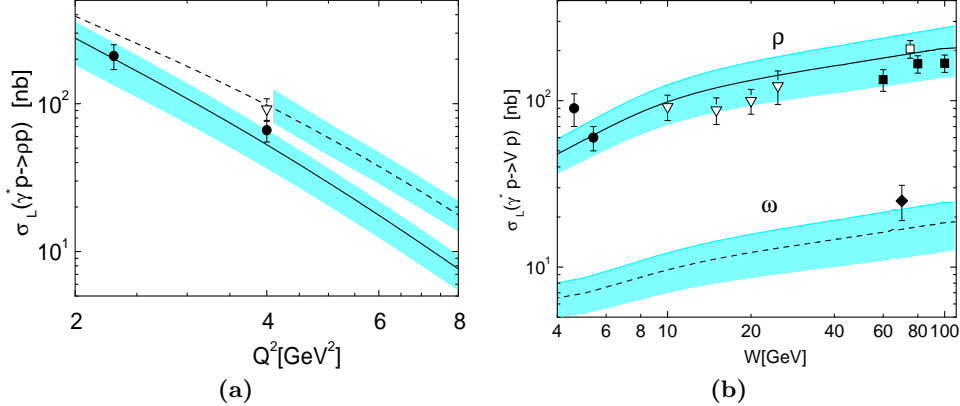


**Fig. 3.** (a) Longitudinal cross sections of  $\rho$  production at  $W = 5 \text{ GeV}$  -full line and  $W = 10 \text{ GeV}$  -dashed line. (b) Energy dependencies of cross section at  $Q^2 = 4 \text{ GeV}^2$ . Full line- longitudinal cross section of  $\rho$  production, dashed line- of  $\omega$  production. Data are from H1 [8]- solid squares, ZEUS [9] - open square and solid diamond [16], E665 [11]- open triangles, HERMES [10] - solid circles,

extremely important at low  $Q^2$ . They decrease the cross section by a factor of about 10 at  $Q^2 \sim 3 \text{ GeV}^2$ .

In Fig. 3a, the cross section for the  $\rho$  production at HERMES ( $W = 5 \text{ GeV}$ ) and our prediction for COMPASS ( $W = 10 \text{ GeV}$ ) are presented. It can be seen that we describe properly the available HERMES data [10] and E665 data at  $W = 10 \text{ GeV}$  [11]. In Fig 3.b, we show the energy dependence of the cross section for the light meson production. At high energies  $W > 10 \text{ GeV}$ , its energy dependence is controlled by the gluon + sea contributions. At lower energies valence quarks are essential. For the  $\rho$  production at HERMES  $W = 5 \text{ GeV}$  the valence quark contribution to the cross section is about 40%. For the case of  $\omega$  production [16] the quark contribution in this energy range is about 65%. This results in a more smooth energy behavior of the  $\omega$  cross section with respect to the  $\rho$  one at  $W \sim 5 \text{ GeV}$ , Fig. 3b.

The TT amplitude, which is essential for spin observables, is calculated here at high energies where we study the gluon contribution only. The analyses of quark effects in the TT amplitude can be found in [3]. We compare our results for spin observables with experimental data at HERA energies where the valence quarks are not essential. The results for the ratio of the cross

section with longitudinal and transverse photon polarization

$$R = \frac{\sigma_L}{\sigma_T} \quad (10)$$

for the  $\rho$  and  $\phi$  production are shown in Fig.4. We describe properly available data from H1 and ZEUS experiments [8,9].

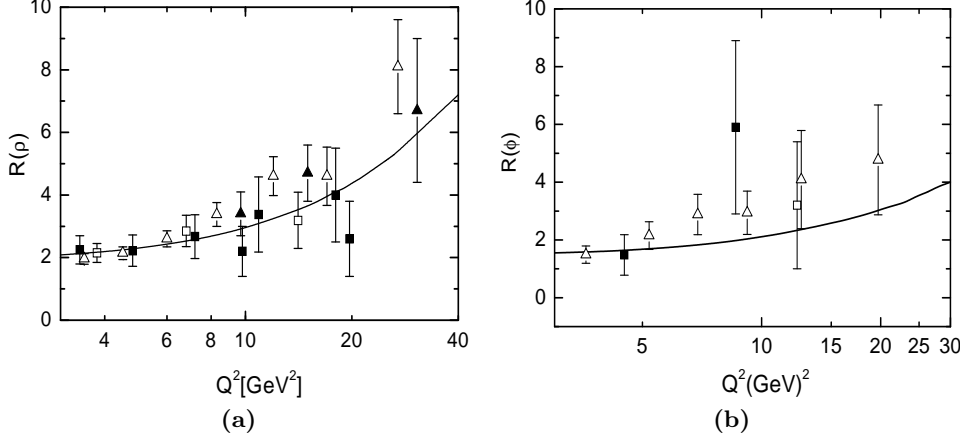


**Fig. 4.** (a)  $R$  ratio of  $\rho$  production at  $W = 75$  GeV. (b)  $R$  ratio of  $\phi$  production at  $W = 75$  GeV. Data are from H1 and ZEUS.

There are a few spin density matrix elements which are sensitive to the LL and TT amplitudes. Three SDME are determined in terms of the  $R$ -ratio. In our approximation, we have

$$1 - r_{00}^{04} = 2 r_{1-1}^1 = -2 \text{Im } r_{1-1}^2 = \frac{1}{1 + \epsilon R}. \quad (11)$$

Two SDME are expressed in terms of the LL and TT amplitudes interference

$$\text{Re } r_{10}^5 = -\text{Im } r_{10}^6 \propto \text{Re}(M_{TT} M_{LL}^*). \quad (12)$$

These SDME are relevant to the phase shift between these amplitudes  $\delta_{LT}$ . In Fig.5, we present our results for the SDME in the DESY energy range. Description of experimental data is reasonable. Note that our model gives small  $\delta_{LT} \sim 2 - 3^\circ$  [1].

## 4 Conclusion or Summary

Light vector meson electroproduction at small  $x$  was analyzed within the handbag model where the amplitude factorizes into a hard subprocess and GPDs. The transverse quark momenta which were considered in the hard propagators and in the vector meson wave function regularize the end-point singularities in the amplitudes with transversally polarized photons. This give a possibility to calculate the TT amplitude and study spin effects in the vector meson production in our model. The  $k_\perp^2/Q^2$  corrections in the propagators decrease the cross section by a factor of about 10 at  $Q^2 \sim 3$  GeV $^2$ . As a result, we describe the cross section at  $Q^2 \geq 3$  GeV $^2$ .

In the model, a good description of the cross section from HERMES to HERA energies [2] is observed. It is found that the gluon and sea contributions control the amplitude behaviour

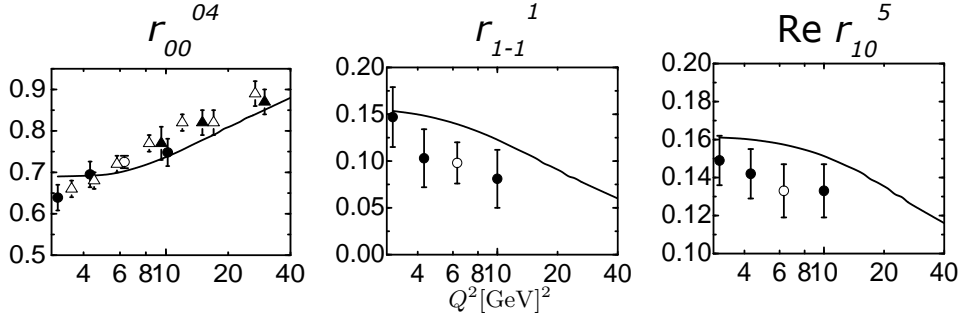


**Fig. 5.** The  $Q^2$  dependence of SDME on the  $\rho$  production at  $t = -0.15 \text{ GeV}^2$  and  $W = 75 \text{ GeV}$ . Data are taken from H1 and ZEUS.

at energies  $W \geq 10 \text{ GeV}$ . Valence quarks are essential only at HERMES energies, where their contribution to  $\rho(\omega)$  cross section is about 40(65)%.

The model describes properly spin effects including the  $R$  ratio and SDME for the light meson production at HERA energies [1]. We would like to point out that study of SDME gives important information on different  $\gamma \rightarrow V$  hard amplitudes. The data show a quite large phase difference  $\delta_{LT} \sim 20 - 30^\circ$  [10]. Our model with a small phase difference  $\delta_{LT}$  gives a reasonable description of experimental data at HERA. Unfortunately, the data on spin observables have large experimental errors. To make clear this and other problems, new experimental results on SDME are extremely important.

Thus, we can conclude that the vector meson photoproduction at small  $x$  is an excellent tool to probe gluon and quark GPDs.

This work is supported in part by the Russian Foundation for Basic Research, Grant 06-02-16215 and by the Heisenberg-Landau program.

## References

1. S.V. Goloskokov, P. Kroll, Euro. Phys. J. C**50**, (2007) 829.
2. S.V. Goloskokov, P. Kroll, Euro. Phys. J. C**42**, (2005) 281.
3. S.V. Goloskokov, P. Kroll, arXiv:0708.3569 [hep-ph].
4. X. Ji, Phys. Rev. D**55**, (1997) 7114;  
A.V. Radyushkin, Phys. Lett. B**380**, (1996) 417;  
J.C. Collins, *et al.*, Phys. Rev. D**56**, (1997) 2982.
5. L. Mankiewicz, G. Piller and T. Weigl, Eur. Phys. J. C**5**, (1998) 119.
6. L. Mankiewicz and G. Piller, Phys. Rev. D**61**, (2000) 074013;  
I.V. Anikin and O.V. Teryaev, Phys. Lett. B**554**, (2003) 51.
7. J. Botts and G. Sterman, Nucl. Phys. B**325**, (1989) 62.
8. C. Adloff *et al.* [H1 Collaboration], Eur. Phys. J. C**13**, (2000) 371;  
C. Adloff *et al.* [H1 Collaboration], Phys. Lett. B**483**, (2000) 360.
9. J. Breitweg *et al.* [ZEUS Collaboration], Eur. Phys. J. C**6**, (1999) 603;  
S. Chekanov *et al.* [ZEUS Collaboration], Nucl.Phys. B**718**, (2005) 3.
10. A. Airapetian *et al* [HERMES collaboration], Eur. Phys. J. C**17**, (2000) 389;  
A. Borissov, [HERMES collaboration], "Proc. of Diffraction 06", PoS (DIFF2006), 014.
11. M. R. Adams *et al.* [E665 Collaboration], Z. Phys. C **74**, (1997) 237.
12. J. Bolz, J.G. Körner and P. Kroll, Z. Phys. A**350**, (1994) 145.
13. I. V. Musatov and A. V. Radyushkin, Phys. Rev. D**61**, (2000) 074027.
14. J. Pumplin, *et al.*, JHEP **0207**, (2002) 012.
15. A. V. Vinnikov, hep-ph/0604248.
16. J. Breitweg *et al.* [ZEUS Collaboration], Phys. Lett. B**487**, (2000) 273.